arXiv:1404.7727v2 [cond-mat.stat-mech] 27 Nov 2014

Active Brownian Particles Escaping a Channel in Single File

Emanuele Locatelli*
Dipartimento di Fisica e Astronomia 'G. Galilei' and Sezione CNISM, Università di Padova, Via Marzolo 8, I-35131 Padova, Italy

Fulvio Baldovin†
Dipartimento di Fisica e Astronomia 'G. Galilei', Sezione INFN, and Sezione CNISM, Università di Padova, Via Marzolo 8, I-35131 Padova, Italy

Enzo Orlandini‡
Dipartimento di Fisica e Astronomia 'G. Galilei', Sezione INFN, and Sezione CNISM, Università di Padova, Via Marzolo 8, I-35131 Padova, Italy

Matteo Pierno§
Dipartimento di Fisica e Astronomia 'G. Galilei' and Sezione CNISM, Università di Padova, Via Marzolo 8, I-35131 Padova, Italy

(Dated: December 1, 2014)

Active particles may happen to be confined in channels so narrow that they cannot overtake each other (Single File conditions). This interesting situation reveals nontrivial physical features as a consequence of the strong inter-particle correlations developed in collective rearrangements. We consider a minimal model for active Brownian particles with the aim of studying the modifications introduced by activity with respect to the classical (passive) Single File picture. Depending on whether their motion is dominated by translational or rotational diffusion, we find that active Brownian particles in Single File may arrange into clusters which are continuously merging and splitting (*active clusters*) or merely reproduce passive-motion paradigms, respectively. We show that activity convey to self-propelled particles a strategic advantage for trespassing narrow channels against external biases (e.g., the gravitational field).

PACS numbers: 64.75.Gh, 47.63.Gd, 47.57.eb

I. INTRODUCTION

The study of the physical properties of living matter has received great attention in the last decade. Beside the relevance in Biology, Physiology and Medicine, these systems can show intriguing new Physics. In particular, active or self-propelled particles (SPP) – individual units that can transform chemical energy into kinetic energy – exhibit a wealth of non-equilibrium phenomena, like collective motion [1], dynamical patterns formation [2–4], and unusual rheological properties [5]. Examples of SPP are microbes and bacteria [6], algae [7], molecular motors [8], but also artificial colloidal microswimmers can be designed to achieve reliable and reproducible examples of self-propulsion [9]. In physically- and biologically-relevant situations [10–16], SPP can be constrained to move in channels so narrow that the mutual passage of the constituents is prohibited. Whenever this happens we say that they form an *Active Single File* (ASF) system. It is known that extreme confinement conditions in passive systems generate strong inter-particle correlations, leading to subdiffusion [17–20]. Under strong confinement as well as biases imposed by external fields or environmental conditions, the enhanced mobility characteristic of active particles may lead to new collective dynamical properties. These, in turns, may strongly affect the the system's transport behavior, e.g., in channel-emptying processes, or the microbiology of soil during infections or for filtration and purification applications [10].

Although hydrodynamic effects are expected to play a role under severe geometric constraints [21, 22], in favor of simplicity and analytical tractability in the present context we consider a minimal Brownian model for active motion [23]. Indeed, a major goal in this work is to study how Single File properties are modified when self-propelled particles are present. We tackle this issue by investigating the interplay between the increased mobility due to activity and the

*Electronic address: emanuele.locatelli@pd.infn.it
†Electronic address: baldovin@pd.infn.it
‡Electronic address: orlandini@pd.infn.it
§Electronic address: matteo.pierno@unipd.it

hindering effects coming from the Single File condition. In particular, with both open channel ends, we concentrate on the dependence of its emptying from either the degree of activity or the rotational vs translational character of the active motion. We find that the active particles undergo a dynamical transition from rotational to translational behavior, which also corresponds to a structural change for the ASF system, with the formation of "active clusters" continuously merging and splitting. Albeit not significantly improved by the existence of clusters, translational active particles expose a significant capability of trespassing channels against external biases.

II. A THEORETICAL MODEL FOR ACTIVE MOTION

On the basis of Ref. [23], we consider a minimal model where 2-dimensional overdamped active particles in contact with a thermal bath are self-propelled by a constant force along a direction specified by an angular coordinate. An active particle of radius R is viewed as characterized by a unit vector $\mathbf{u}(t) \equiv (\cos\theta(t), \sin\theta(t))$ in the xy plane, defining the direction of the active force of intensity F_a. The particle is subjected to both translational and rotational diffusion, with coefficients D_t and D_r, respectively. Once projected along the channel direction, which we assume to coincide with the x-axis, the equations of motion become

$$\begin{cases} \dot{x}(t) = \dfrac{D_t}{k_B T}\left[F_a \cos\theta(t) + F_e\right] + \xi_t(t), \\ \\ \dot{\theta}(t) = \xi_r(t), \end{cases} \tag{1}$$

where k_B is the Boltzmann constant, T the heat-bath temperature, F_e is the external uniform force, and both $\xi_t(t)$ and $\xi_r(t)$ are Gaussian white noise, $\langle \xi_t(t)\,\xi_t(t')\rangle = 2D_t\,\delta(t-t')$, $\langle \xi_r(t)\,\xi_r(t')\rangle = 2D_r\,\delta(t-t')$, representing a random force and a random torque, respectively. In particular, D_t is assumed to satisfy the Einstein relation $\zeta\, D_t = k_B T$ where ζ is the translational friction coefficient that, for a spherical particle of radius R in a fluid with viscosity η is equal to $6\pi R\eta$. The active force is related to the modulus of the drift velocity of the active particle v_a, $F_a = \zeta\, v_a$, in the absence of external fields.

A. Linear vs rotational diffusion: identification of a crossover line

As customary we quantify the particle's activity through the Péclet number, namely the ratio between advection and diffusion [24]:

$$\mathrm{Pe} \equiv \frac{v_a R}{D_t} = \frac{F_a R}{k_B T} \geq 0. \tag{2}$$

Within our model, Pe can also be interpreted as the ratio between the work done by the active force over a distance of the order of the particle's size and the thermal energy. At variance with Ref. [23], we do not fix the ratio between D_r and D_t. Instead, we encode it into a second adimensional parameter,

$$\mathrm{Ro} \equiv R^2 D_r / D_t \geq 0, \tag{3}$$

which we name the *rotation number* and that expresses the predominance of the rotational over the translational diffusion. Equivalently, Ro may be seen as the ratio between the translational and the rotational time scales, $\tau_t = R^2/2D_t$ and $\tau_r = 1/2D_r$, respectively. Pe and Ro can be easily related to other quantities, like, e.g., the persistence length $L_p \equiv v_a/D_r$ which is often used in simulation as a control parameter: Namely,

$$L_p = \frac{\mathrm{Pe}}{\mathrm{Ro}}\, R. \tag{4}$$

The main advantage in using Pe and Ro is that we have two independent control parameters which neatly separate the effects of the activity and of the rotational diffusion on the particle dynamics. In a run-and-tumble model in which the rotational dynamics is typically defined through a shot noise, the rotation number would be defined as $\mathrm{Ro} \equiv R^2\alpha/D_t$, where α is the tumbling rate [25, 26].

Once averaged over a uniform distribution of the initial angles $\theta(0) = \theta_0$, there is no preferred direction for the active motion, and the mean square displacement from the initial position $x(0) = x_0$ evolves as

$$\langle (x(t) - x_0)^2 \rangle = 2D_t t + \frac{\mathrm{Pe}^2}{\mathrm{Ro}^2}\, R^2 \left[D_r t + e^{-D_r t} - 1\right] \tag{5}$$

$$\simeq 2D_a t, \tag{6}$$

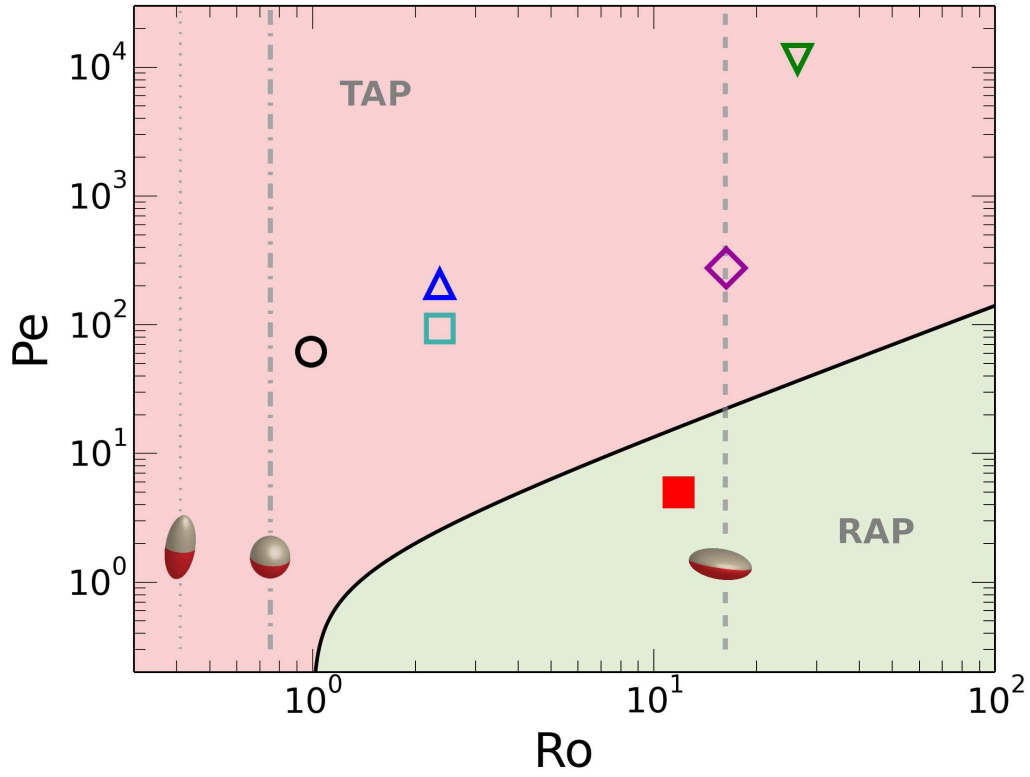

FIG. 1: (Color online) Ro-Pe phase diagram for SPP. The full line, given by Eq. (8) with Ro > 1, distinguishes TAP's from RAP's. Symbols refer to different microorganisms. Circle is *V. Alginolyticus* [27]; Upward triangle is *P. Putida* [28]; Empty square is wild type *E. Coli*; Filled square is RAP mutant *E. Coli* [29]; Diamond is *R. Spheroides* [30]; Downward triangle is *C. Reinhardtii* [31]. Vertical lines represent Janus microswimmers: Prolate Spheroids (dotted); Spheres (dash-dotted); Oblate Spheroids (dashed).

where the last approximation is valid for $t \gg \tau_r$, and we have defined an effective, active diffusion coefficient as

$$D_a \equiv D_t \left(1 + \frac{\mathrm{Pe}^2}{2\,\mathrm{Ro}}\right). \tag{7}$$

Besides τ_t and τ_r, we thus have also an active time scale $\tau_a = R^2/2D_a$. Notice that as a consequence of the random direction of the active force, instead of being related to the drift, τ_a is associated to an active diffusion process.

The influence of the reorientational process on the translational dynamics depends on the typical timescale of the rotational diffusion as well as on the magnitude of the active force. It is thus defined by the ratio between the typical timescales of rotational and translational motion, τ_r and τ_a respectively. For $\tau_a \ll \tau_r$ the motion is dominated by (active) translational diffusion with a predominance of straight trajectories over bends; Vice versa, as $\tau_a \gg \tau_r$ rotational diffusion become prevalent. The condition $\tau_r/\tau_a = 1$ leads to a relation between Péclet and Rotation numbers

$$\mathrm{Pe} = \begin{cases} \mathrm{Ro}\,\sqrt{2\left(1 - \frac{1}{\mathrm{Ro}}\right)} & \text{if } \mathrm{Ro} > 1 \\ 0 & \text{if } 0 \le \mathrm{Ro} \le 1 \end{cases} \tag{8}$$

that is graphically reported in Fig. 1. This relation divides the plane Ro-Pe in two distinct regions and suggests a way to classify the active particles of our model as follows: A Self-Propelled particle may be called *Translational Active Particle – TAP* (*Rotational Active Particle – RAP*) if it lies above (below) the line. Note that compared to their characteristic translational timescale TAP's change the direction of the active force slowly, hence they exhibit long periods of straight motion; On the other hand rotational diffusion is predominant for RAP's dynamics. Although in our case the particle orientation is not abruptly "tumbled" through a shot noise term, we may thus associate TAP's to *runners* and RAP's to *tumblers* with respect to run-and-tumble models [26].

Available data for bacteria and algae indicate that these microorganisms have a tendency to perform long period of straight motion. Consistently, in the Ro-Pe representation they are classified as TAP's (See empty symbols in Fig. 1).

On the other hand, bacteria mutants obtained through genetic engineering may become RAP's (See filled square in Fig. 1). For artificial microswimmers (Vertical lines in Fig. 1), Ro is fixed and depends on the shape, while Pe can be tuned by varying, for example, the H_2O_2 concentration [32]. Eq. (8) is particularly interesting when studying an ASF system. Indeed, in passing from RAP's to TAP's it identifies a crossover line which singles out the formation of dynamical aggregates.

III. ACTIVE BROWNIAN PARTICLES ESCAPING A CHANNEL IN SINGLE FILE

In analogy with passive systems one would expect that interacting Self Propelled particles under Single File condition (ideal representation of an extreme channel-like confinement) display significant changes with respect to the dynamical properties in the bulk. By focusing in particular on the emptying process of the Single File we show that the distinction between RAP's and TAP's determines the main properties of the system such as dynamical clustering and the mean emptying time either in the presence or in the absence of an external bias.

A. Analytical derivation of the channel's emptying probability

To properly address the problem of the emptying process of an active system under Single File constraint it is convenient to look first at the corresponding problem for a system of passive particles. Single File conditions force particles to maintain spatial order thus generating a complex correlation structures in the system. As a result, particles perform a subdiffusive motion which lasts for a very long time if their number is large enough [33]. In spite of this, passive Single File evolution can be mapped onto normal diffusion thanks to the Reflection Principle. It has been Jepsen [34] the first to point out that it is possible to map the Single File diffusion onto a free particles diffusion in which at each collision particles simply exchange their labels. This is equivalent to impose reflecting boundary conditions at the planes $x_i(t) = x_j(t)$ at which particles i and j collide [35].

The combinations of all possible reflections are given by the permutations of the coordinates, so that the probability $P_N(\mathbf{x}, t|\mathbf{x}^0, N, L)$ of finding the Single File array in positions $\mathbf{x} \equiv (x_1, x_2, \ldots, x_N)$ at time t within a channel centered in $x = 0$ of width L, given that the initial coordinates a time zero are $\mathbf{x}^0 \equiv (x_1^0, x_2^0, \ldots, x_N^0)$ with $-L/2 \leq x_1^0 < x_2^0 < \ldots < x_N^0 \leq L/2$, is provided by the expression [35]

$$P_N(\mathbf{x}, t|\mathbf{x}^0, N, L) = \begin{cases} \displaystyle\sum_{\pi \in \Pi_N} \prod_{k=1}^{N} P_1(x_{\pi(k)}, t|x_k^0, 1, L) & \text{if } \mathbf{x} \in \mathcal{D}, \\ \\ 0 & \text{if } \mathbf{x} \notin \mathcal{D}, \end{cases} \tag{9}$$

where Π_N is the set of permutations of N objects, $\mathcal{D}$ represents the set of allowed configurations, $\mathcal{D} \equiv \{\mathbf{x} \in \mathbb{R}^N : -L/2 \leq x_1 < x_2 < \ldots < x_N \leq L/2\}$, and $P_1(x_k, t|x_k^0, 1, L)$ is the Green function for the free single-particle problem with absorbing boundaries at $x = \pm L/2$. Although exact, Eq. (9) is hard to handle both analytically and numerically because of the restriction on the allowed configurations. However, if one is interested in the survival probability of *all* the N particles within the channel,

$$S_N(t|\mathbf{x}^0, N, L) = \int_{\mathcal{D}} d\mathbf{x}\, P_N(\mathbf{x}, t|\mathbf{x}^0, N, L), \tag{10}$$

permutations in Eq. (9) allow to remove the particles order constraint and one obtains

$$S_N(t|\mathbf{x}^0, N, L) = \prod_{k=1}^{N} S_1(t|x_k^0, 1, L), \tag{11}$$

where $S_1(t|x_k^0, 1, L)$ is the survival probability of a single free particle originally posed at x_k^0 and absorbed in $\pm L/2$.

For the study of the emptying process of a Single File system of identical particles Eq. (11) turns out to be a fundamental simplification. If we indicate with $S_n(t|\mathbf{x}^0, N, L)$ the probability of having *at least* $0 \leq n \leq N$ particles within the channel at time t, given that initially N particles are posed in position $\mathbf{x}^0 \equiv (x_1^0, x_2^0, \ldots, x_N^0)$ within a channel of length L, the channel emptying probability becomes

$$1 - S_1(t|\mathbf{x}^0, N, L). \tag{12}$$

Now, $S_n(t|\mathbf{x}^0, N, L)$ can be viewed as the sum

$$S_n(t|\mathbf{x}^0, N, L) = \sum_{k=n}^{N} p_k(t|\mathbf{x}^0, N, L), \tag{13}$$

where $p_n(t|\mathbf{x}^0, N, L)$ is the probability of having n particles within the channel at time t, given that at time zero the N particles were located at $\mathbf{x}^0$. Another way of defining $p_n(t|\mathbf{x}^0, N, L)$ is by saying that n particles have a first passage time at the boundaries larger than t, while for $N-n$ ones the first passage time is smaller than t. Thanks to Eq. (11) we thus have

$$\begin{aligned} p_n(t|\mathbf{x}^0, N, L) =& \frac{1}{n!\,(N-n)!} \sum_{\pi\in\Pi_N} \int_t^\infty dt_1 \cdots \int_t^\infty dt_n \\ & \int_0^t dt_{n+1} \cdots \int_0^t dt_N \prod_{k=1}^{N} \left[-\frac{dS_1(t_k|x^0_{\pi(k)}, 1, L)}{dt_k} \right] \\ =& \frac{1}{n!\,(N-n)!} \sum_{\pi\in\Pi_N} \prod_{k=1}^{n} S_1(t|x^0_{\pi(k)}, 1, L) \prod_{k=n+1}^{N} [1 - S_1(t|x^0_{\pi(k)}, 1, L)], \end{aligned} \tag{14}$$

where the combinatorial factors again arise as a consequence of the particles exchange symmetry. If the initial conditions $\mathbf{x}^0$ are randomly distributed along the channel, all the single-particle survival probabilities in Eq. (14) become equal and Eq. (13) neatly simplifies into

$$S_n(t|N, L) = \sum_{k=n}^{N} \binom{N}{k} S_1(t|1, L)^k \, [1 - S_1(t|1, L)]^{N-k}, \tag{15}$$

where

$$S_1(t|1, L) \equiv \frac{1}{L} \int_{-L/2}^{L/2} dx_k^0 \;\; S_1(t|x_k^0, 1, L) \tag{16}$$

is the survival probability of a free particle initially placed at random within the channel. To the best of our knowledge, we are accounting here the first analytical derivation of Eq. (15), which governs the escape dynamics of passive particles in Single File. In particular, the channel emptying probability becomes

$$1 - S_1(t|N, L) = 1 - \sum_{k=1}^{N} \binom{N}{k} S_1(t|1, L)^k \, [1 - S_1(t|1, L)]^{N-k} \tag{17}$$

Integrating Eq. (17) over time gives the mean emptying time:

$$T_1(N, L) = \int_0^\infty dt \; S_1(t|N, L). \tag{18}$$

B. Unbiased channel emptying for active Brownian particles

When activity is introduced, the interplay between rotational and translational timescales has some important consequences. After a collision two TAP's will tend to push one against the other, promoting the formation of a small aggregate of swimmers. Thus, collisions among TAP's may be seen as non-reflecting collisions; In turns, the the reflection principle could be effectively preserved in collisions among RAP's. As a consequence, Eqs. (15,18) are expected to play a role also in the realm of ASF systems, but only below the crossover line established in Eq. (8).

As specified in the Appendix, we performed simulations for different values of Ro and Pe. A quantitative way of addressing the significance of Eqs. (15,18) is by monitoring the the relative difference of the numerical mean emptying time $T_1^{(num)}(N, L)$ with the theoretical result $T_1(N, L)$,

$$\delta(N, L) \equiv \frac{T_1^{(num)}(N, L) - T_1(N, L)}{T_1^{(num)}(N, L)}, \tag{19}$$

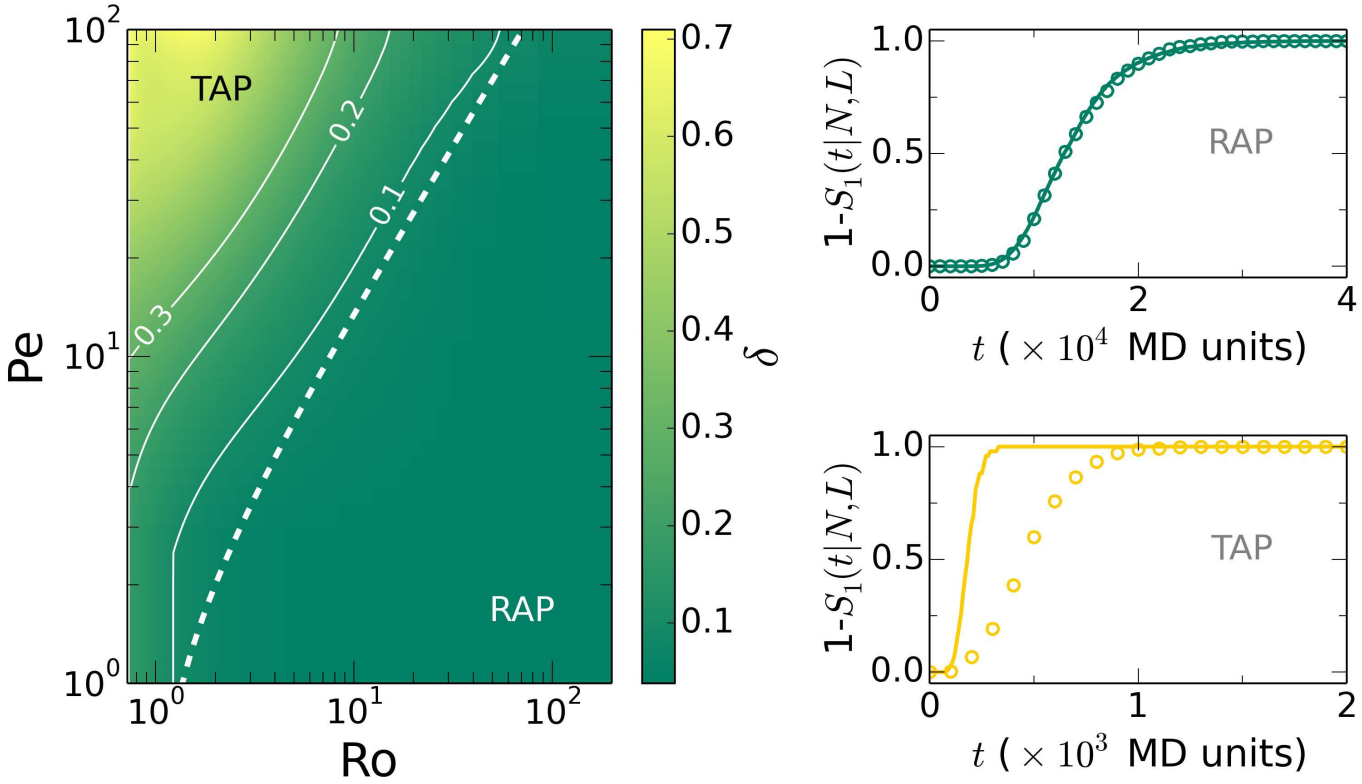

FIG. 2: (Color online) Left panel: Ro-Pe phase diagram for the emptying process of an ASF system. Level curves refer to the relative difference $\delta(N, L)$ in Eq. (19) for $N = 21$ and $L = 52$ (MD units). The dashed curve, given by Eq. (8), distinguishes TAP's (above) from RAP's (below). Right panels: Emptying probability $1 - S_1(t|N, L)$ for a RAP (Ro = 200, Pe = 50) and a TAP (Ro = 0.75, Pe = 50). Circles are numerical simulations, lines are obtained through Eq. (15).

where the survival probability $S_1(t|1, L)$ in Eq. (15) has been numerically determined. The level curves plots reported in Fig. 2 show that, indeed, below the line in Eq. (8) δ is small and the agreement with Eqs. (15,18) is remarkable for RAP's (See also top-right panel). As we move deeper in the TAP's region, δ grows of few percents and deviations with Eqs. (15,18) become sensible (Compare also with the bottom-right panel).

C. Dynamical clustering in Single File

The validity-range of Eqs. (15,18) also corresponds to a structural change in ASF systems. Collisions can be understood as seeds for the nucleation of dynamical clusters held together by the action of active forces. Consider (active) hardcore particles of radius $\sigma/2$. The presence of peaks at separation multiple of σ in the static, distinct radial distribution function,

$$G_2(x) \equiv \frac{1}{N} \left\langle \sum_{i \neq j} \delta \left(x - x_j + x_i \right) \right\rangle , \tag{20}$$

reveals the existence of clusters, with the number of peaks corresponding to the typical cluster-size in units of σ. We numerically studied G_2 for an ASF system, this time with periodic boundary conditions to increase our sampling. Ensemble averages at a time much larger than the system's correlation time are obtained by considering the particles' coordinates x_i and x_j in different dynamical realizations with random initial conditions. Level curves in Fig. 3, which report the number of peaks of G_2 as a function of Ro and Pe, retain a close similarity with Fig. 2. This means that RAP's do not aggregate, whereas TAP's do. Hence, the line in Eq (8) also marks the onset of dynamical clustering where SPP's continuously merge and split into coherent assemblies. Note that dynamical clustering has been observed and discussed very recently in several examples of self-propelled particle systems, in one, two and three dimensions [36–42]. In the following we show that this collective effect however does not improve the chances of a single TAP to escape the channel against an external bias.

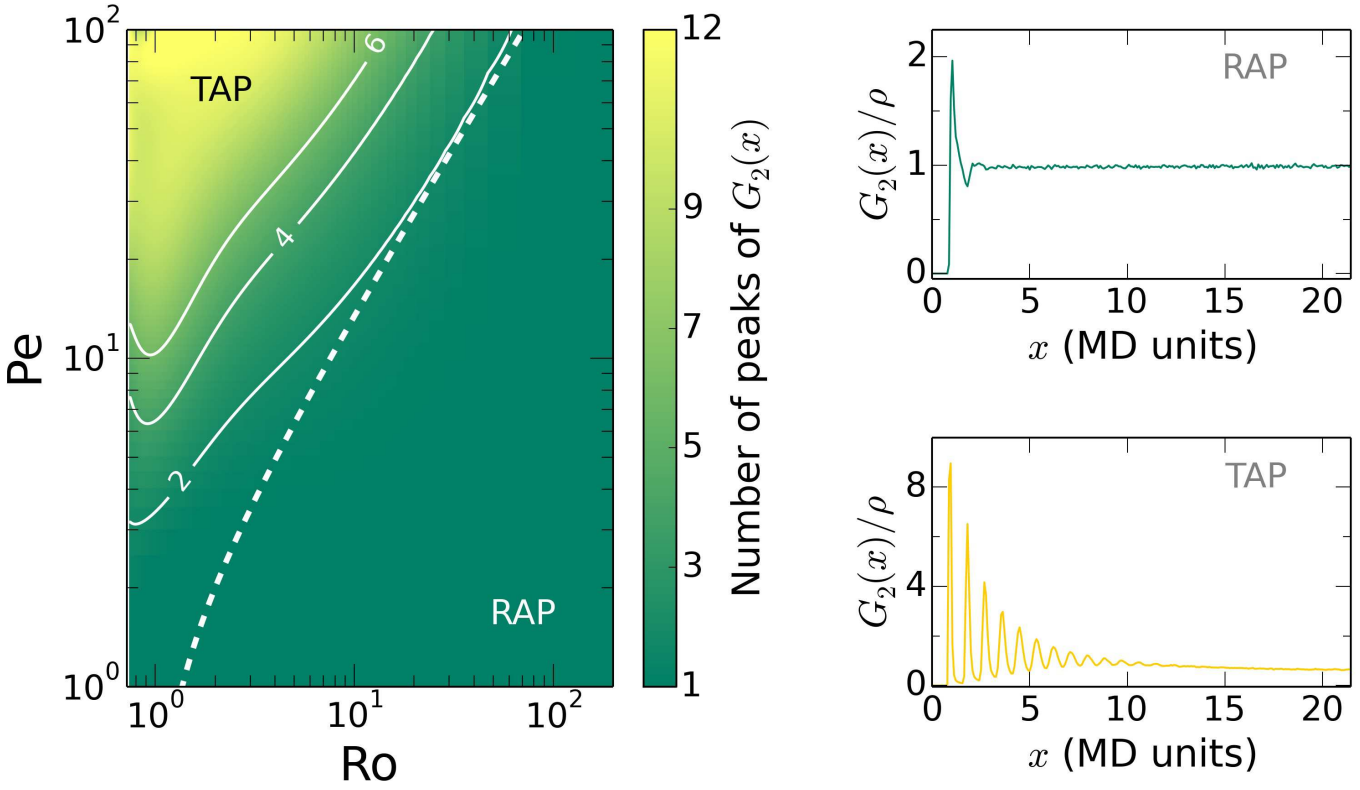

FIG. 3: (Color online) Left panel: Phase diagram of the number of peaks of $G_2(x)$ for ASF systems. $N = 21$ hardcore particles of radius $R = 0.5$ and number density $\rho = N/L = 0.5$, are simulated with periodic boundary conditions. The dashed curve, given by Eq. (8), distinguishes TAP's (above) from RAP's (below). Full lines are level curves. Right panels: radial distribution functions for RAP's (Ro = 200, Pe = 50) and TAP's (Ro = 0.75, Pe = 50).

D. Emptying process in the presence of an external bias

An interesting practical situation is that of biased or "tilted" Single File channels. In several biological processes as well in microfluidic devices SPP's may be found to move against the direction of an externally imposed bias (e.g., the gravitational field [43, 44]). We explore this problem by adding to our ASF model an external constant and uniform force field F_e pointing along the channel direction, say, to its right end. Even within this extended parameter space (enlarged by the presence of the field), the previous distinction between TAP's and RAP's highlights different dynamical behaviors.

We start the characterization of the emptying process for tilted channels by studying the existence of possible correlations among the active force orientations. Specifically, at the instant at which a particle leaves the channel from the left (against the bias), we calculate the average $\langle \cos\theta \rangle$ (θ being the angle between the active force orientation and the channel axis) for those particle still in the channel that appear to be part of a cluster. We consider a particle to part of a cluster if one of its nearest neighbor is closer than the interaction range (See Appendix A). The average is both over the different particles satisfying such a condition and over different escaping events. With this definition we can collect a good statistics for both TAP's and RAP's. In the latter case this happens because, although no stable cluster is formed, within the channel there are enough colliding particles which are forming an instantaneous two-particle cluster for the average to be significantly calculated. In Fig. 4 we show that at low Ro $\langle \cos\theta \rangle$ is smaller than zero, meaning that at the instant when a particle leaves the channel against the bias clustered TAP's in the channel tend to point along the left. Increasing Ro towards RAP's particles, this tendency is lost. This observation is consistent with the fact that the "active clusters" detected in the previous Section tend in fact to have a common orientation of the active force at the moment a particle exits against the bias. Hence, particles in a cluster leave the channel one after the other in a rapid sequence (See animations in the Supplementary Material). This effect, which also exists in the absence of the bias ($F_e = 0$), gets weaker as F_e increases, and vanishes for $F_e \gtrsim F_a$. Under the latter circumstances, trespassing the channel against the bias becomes a rare, isolated event.

We now focus on the capability of particles, initially randomly distributed both in space and velocity direction, to overcome the external bias. A quantitative measure of such a capability is given by (twice) the fraction of particles

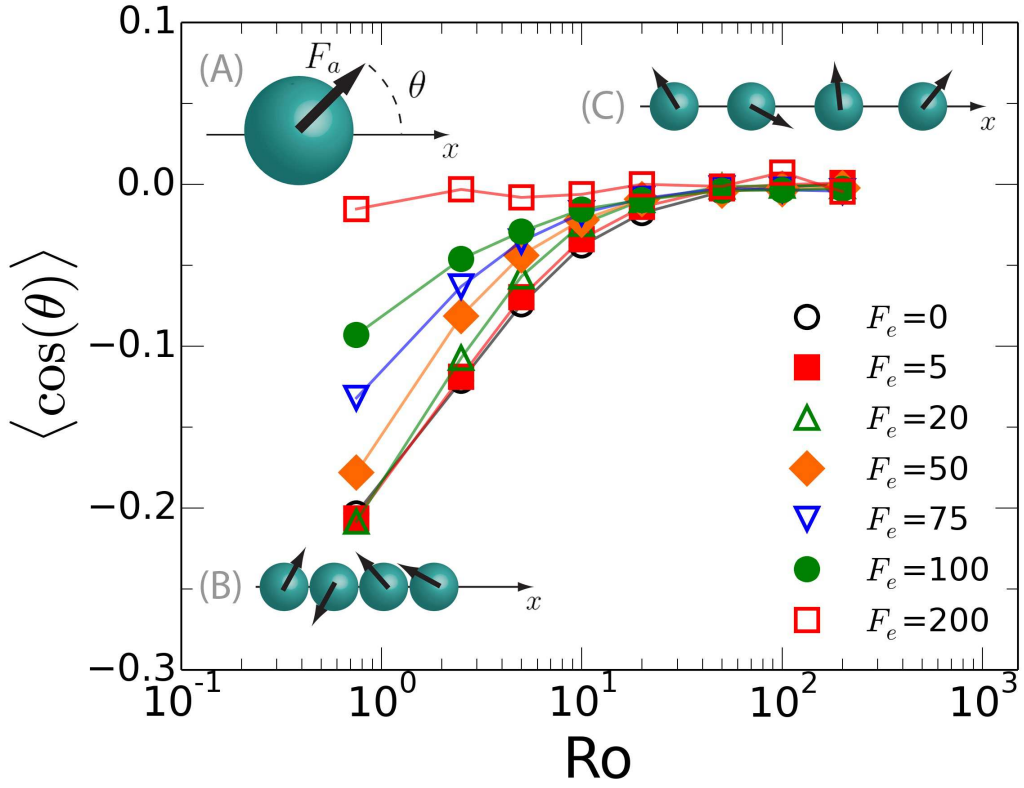

FIG. 4: (Color online) Average direction of the clustered self-propelled particles at the instant in which a particle exits the channel from the left. F_e (in MD units) is the external force pointing to the right and θ is the angle between the active force orientation and the channel axis oriented to the right. The Péclet number is Pe = 100 and $N = 21$. (A) Sketch of the active particle model described in Section II. (B) TAP's leaving the channel against the bias F_e form dynamically correlated clusters. (C) At variance, RAP's are uniformly dispersed with an active force with a randomly distributed orientation. (See animations in the Supplementary Material).

exiting on the left side of the channel,

$$\phi_l(\mathrm{Ro}, \mathrm{Pe}, F_e) \equiv 2\, \frac{\langle N_l(\mathrm{Ro}, \mathrm{Pe}, F_e)\rangle}{N}, \tag{21}$$

where $\langle N_l \rangle$ is the average number of particles absorbed at the left end. With the inclusion of the factor 2 in Eq. (21), the value $\phi_l = 1$ indicates that on average half of the particles leave the channel from the left side and the emptying process is not affected by F_e. On the other hand, when $\phi_l = 0$ no particle is capable to overcome the bias. The left panel of Fig. 5a displays results of numerical simulations performed for 21 at Pe = 100, a typical value for several microswimmers. Again, by increasing Ro we observe a significant change of ϕ_l. Whereas TAP's retain a significant capability of moving against the external bias even under Single File conditions, RAP's are dominated by the force field. Given the similarity of the ϕ_l curves with respect to different biases in the left panel of Fig. 5a, it is interesting to check whether the SPPs exhibit a common way to trespass the channel against a given F_e. Intriguingly, by comparing the typical energy of the SPP with the energy barrier imposed by the external bias, the fraction of upstreamers ϕ_l turns out to satisfy a scaling behavior whenever $F_a < F_e$. More precisely if, for given values of Pe and F_e, we divide ϕ_l by its maximum value $\phi_l{}^{\max}(\mathrm{Pe}, F_e) = \phi_l(\mathrm{Ro} \simeq 0, \mathrm{Pe}, F_e)$, we obtain the fraction $\phi_l^\star$ of upstreamers with respect to the fraction of TAP's (Ro $\simeq 0$),

$$\phi_l^\star(\mathrm{Ro}, \mathrm{Pe}, F_e) \equiv \frac{\phi_l(\mathrm{Ro}, \mathrm{Pe}, F_e)}{\phi_l(0, \mathrm{Pe}, F_e)} = f\left(\frac{W_e}{W_a}\right), \tag{22}$$

where

$$W_e \equiv F_e\ L/2, \qquad \text{and} \qquad W_a(\mathrm{Pe}, \mathrm{Ro}) \equiv k_B T \left[1 + \frac{\mathrm{Pe}^2}{2\,\mathrm{Ro}}\right] = k_B T\ \frac{D_a}{D_t}. \tag{23}$$

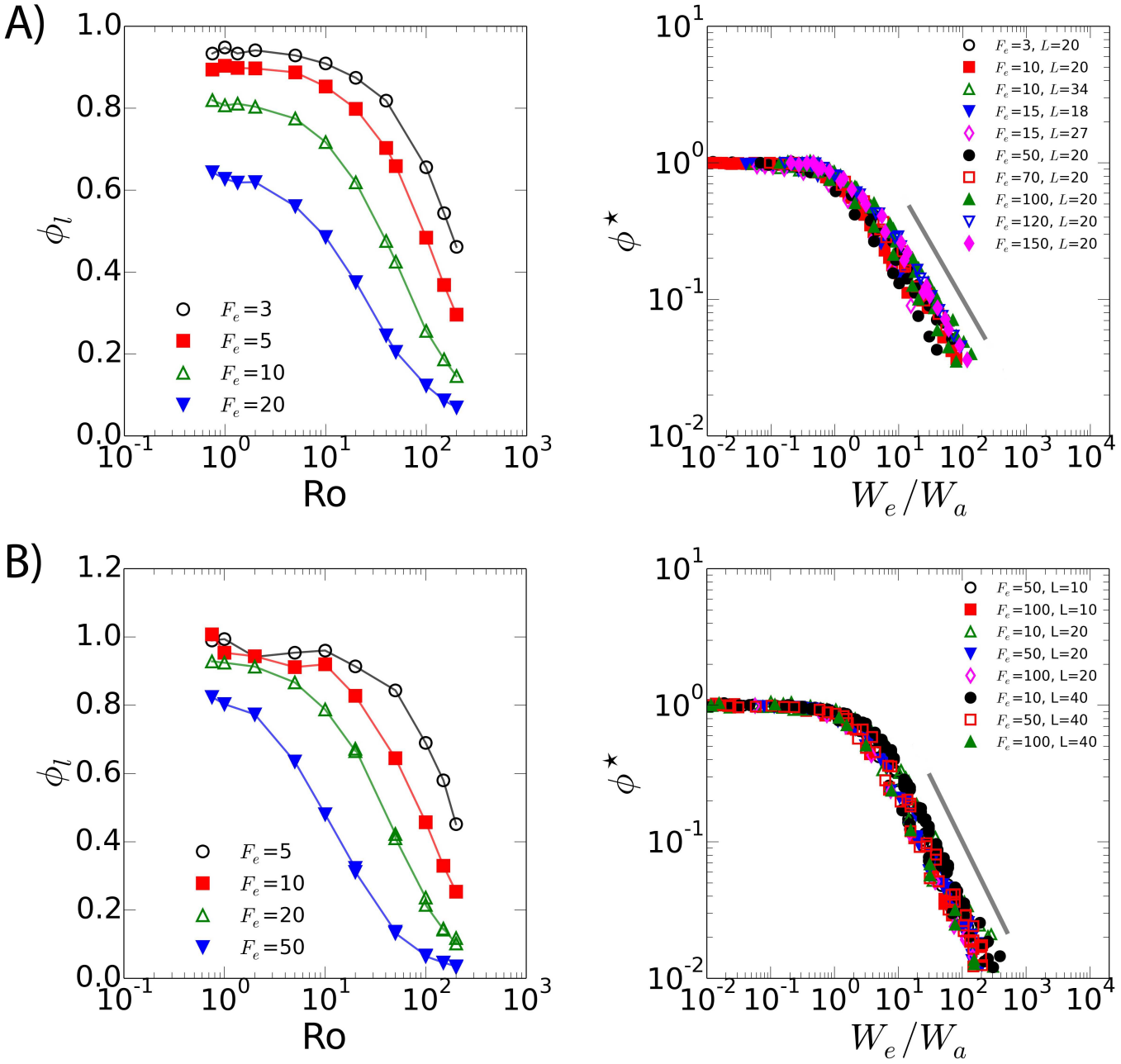

FIG. 5: (Color online) A) Left panel: capability of ASF particles to overcome external biases F_e (in MD units). The Péclet number is Pe = 100 and $N = 21$. Right panel: scaling symmetry characterizing $\phi^\star$ (See text for details). The straight line highlights a power law decay with an exponent of about 0.75. B) Same as A) with $N = 1$. The straight line in the right panel has an exponent of about 0.95.

Notice that W_e and W_a can be understood respectively as the average work done by the external force to bring a SPP out of a channel of length L, and the effective thermal energy for a SPP at given values of Pe and Ro. The right panel of Fig. 5a indeed exhibits a data-collapse of simulations performed at different values of Ro, Pe, F_e, L. The master curve f in Eq. (22) shows an initial very slow decay which crosses over to a power-law regime. In particular, $\phi^\star$ remains close to 1 for TAP's (small Ro and thus large W_a). The existence of these two regimes demonstrate the specific capability of TAP's of being better resilient to the imposed field. Moreover, the collapse of the data into a single master curve f suggests that, whenever a confined system fulfills Single File conditions, a common (universal) behavior for SPP's (either TAP's or RAP's) is expected regardless of their, dimensions or propelling mechanism. We believe this conclusion to be worth further inspected through experimental tests.

One may speculate whether the existence of clusters of TAP's improves the chances of trespassing the channel

against the bias. Fig. 5b demonstrates that this is not the case. Essentially the same behavior obtained for $N = 21$ in Fig. 5a is reproduced in Fig. 5b for $N = 1$. For the system sizes we have analyzed, this means that the capability of TAP's of moving against the bias is simply a consequence of their "translational activity" and is not a cooperative effect.

IV. CONCLUSION

In this paper we have studied the dynamical properties of active particles under Single File conditions, an ideal representation of a very narrow channel in which particles cannot pass each other. Within a simple model of self-propelled particles we have proposed a characterization of their dynamics by introducing, besides the Péclet number Pe, the *rotation* number Ro. Although instrumental to our scopes, Ro is simply related to other quantities (like the particles' persistence length) so that equivalent ways of characterizing the translational-to-rotational character of the active particles are possible. According to our scheme, particles can be distinguished into TAP's and RAP's, separated by Eq. (8) in the Ro-Pe phase space. By examining data reported in the literature we find that most bacteria and algae, even if characterized by a rotation number Ro larger than that of spherical Janus particle, remain above the crossover line and behave as TAP's. The distinction between RAP's and TAP's turns out to be important in investigating some dynamical properties of active particles in Single File such as the emptying process of a narrow channel with and without an external bias. In particular, we have shown that analytical tools here introduced to characterize passive motion can be also used to describe RAP's emptying process of the channel. Unlike RAP's the main distinctive property of TAP's is their aptness to form aggregates, named "active clusters". Although not in consequence of a cooperative effect, TAP's have been also shown to possess higher capabilities of trespassing narrow channels against external fields.

Since our main goal has been to discuss within a simple picture how classic Single File emptying processes are altered by the presence of activity, throughout our study hydrodynamic interactions have been neglected. These might be relevant especially in the case of bacteria and algae. In particular, while for a single cell the hydrodynamic effect due to extreme confinement could be neglected [10], cell-cell interactions in crowded systems may be influenced by hydrodynamics [21]. These last aspects are certainly worth to be explored in the future, either experimentally or theoretically. On the other hand, in cases in which physical interactions could be dominated by steric rather than hydrodynamic contributions, our findings are to be interpreted as a strategic advantage for TAP's microorganisms in overcoming external biases in strongly confined environment, leading to better chances in food search, environment exploration or propagation of infections. In this view it is interesting to notice that genetic mutation may transform TAP's into RAP's, thus, in principle, drug therapies increasing Ro by enhancing the rotational diffusion could eliminate such an advantage.

Acknowledgments

We gratefully acknowledge financial support from the European Research Council under the European Community's Seventh Framework Programme (FP7 2007-2013) / ERC Grant Agreement N. 297004 (DREOEMU), and from the University of Padova (PRAT 2013 N. CPDA138901). In addition the authors kindly thank Prof. U. Keyser, Dr. S. Pagliara and Dr. P. Cicuta, from the University of Cambridge, for useful discussions.

Appendix A: Numerical simulations

We briefly describe the numerical schemes used in our simulations. We adopted natural Molecular Dynamics units for length, mass, and time, with $k_B = 1$. Between the collisions, we use a simple Brownian Dynamics scheme:

$$\begin{cases} x(t+\Delta t) = x(t) + \dfrac{D_t}{k_B T}\left(F_a \cos(\theta(t)) + F_e\right)\Delta t + \sqrt{\Delta t}\,\xi_t(t), \\ \\ \theta(t+\Delta t) = \theta(t) + \sqrt{\Delta t}\,\xi_r(t), \end{cases} \tag{A1}$$

where $R = 0.5$, $D_t = 0.01$, D_r is fixed by the specific value of Ro considered, T=1 is the temperature of the heath bath, m=1 is the particle mass and $\Delta t = 10^{-3} - 10^{-4}$ is the elementary time-step. The random noises $\xi_t(t)$ and $\xi_r(t)$ are normal independent pseudo-random numbers. $F_a \in [1, 300]$ and $F_e \in [0, 300]$ are the constant active and external forces, respectively. We performed simulations with both periodic and absorbing boundary conditions. In

the case of periodic boundaries the elapsing simulation time has been $10^6\Delta t$, while with absorbing boundaries it has been variable in the range $[10^4\,\Delta t, 10^7\,\Delta t]$; In both cases, from 10^3 to 10^6 independent realizations were performed.

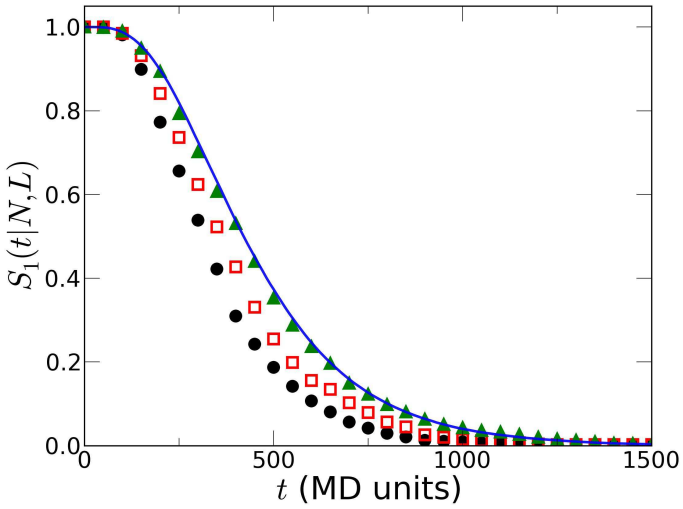

FIG. 6: (Color online) Emptying probability $S_1(t|N,L)$ obtained using the two simulation methods described in the text, for N=5 particles, L=12 (MD units), Pe=50 and Ro=200. The full line is the result of the point-like scheme, while the symbols are the result of the truncated-shifted Lennard-Jones scheme. Different values of σ are employed: full dots for σ=1, open squares for σ=0.5, full triangles for σ=0.1.

To simulate collisions between point-like particles, whenever they overtake each other we switch the labels of the colliding particles returning thus to their pre-collision ordering. Conversely, to study the phenomenon of dynamical aggregation we simulate particles with a certain size σ, employing a truncated-shifted Lennard-Jones interaction potential [45]:

$$U_{ij} = \begin{cases} 4\epsilon\left[\left(\frac{\sigma}{r_{ij}}\right)^{12} - \left(\frac{\sigma}{r_{ij}}\right)^{6}\right] + \epsilon & r_{ij} < \sigma\, 2^{1/6}, \\ 0 & r_{ij} \geq \sigma\, 2^{1/6}. \end{cases} \tag{A2}$$

Specifically, we have chosen σ=1. This two simulation methods give the same results in the dilute limit $L/\sigma \to \infty$, which can be achieved letting $\sigma \to 0$ with a fixed L. Fig. 6 compares the emptying probabilities obtained using the two simulation methods. Indeed, for $\sigma \to 0$ the second method gives the same result of the first.

References

[1] T. Vicsek and A. Zafiris, Phys. Rep. **517**, 71-140 (2012).
[2] M.E. Cates, D. Marenduzzo, I. Pagonabarraga, and J. Tailleur, Proc. Nat. Acad. Sci. **107**, 11715 (2010).
[3] L. Berthier and J. Kurchan, Nature Physics **9**, 310-314 (2013).
[4] H.H. Wensink, J. Dunkel, S. Heidenreich, K. Drescher, R.E. Goldstein, H. Löwen and J.M. Yeomans, Proc. Nat. Acad. Sci. **109**, 14308-14313 (2012).
[5] Y. Hatwalne, S. Ramaswamy, Madan Rao and R. Aditi Simha, Phys. Rev. Lett. **92**, 118101 (2004).
[6] Berg H.C., *E. Coli In Motion* (Springer, New York, 2004).
[7] M. Polin, I. Tuval, K. Drescher, J.P. Gollub and R.E. Goldstein, Science **325**, 487 (2009).
[8] T. Surrey, F. Nédélec, S. Leibler and E. Karsenti, Science **292**, 11671171 (2001).
[9] W.F. Paxton, K.C. Kistler, C.C. Olmeda, A. Sen, S.K. St. Angelo, Y. Cao, T.E. Mallouk, P.E. Lammert and V.H. Crespi, J. Am. Chem. Soc. **126**, 13424-13431 (2004).
[10] J. Mannik, R. Driessen, P. Galajda, J.E. Keymer and C. Dekker, Proc. Nat. Acad. Sci. **106**, 14861-14866 (2009).
[11] S.A. Biondi, J.A. Quinn and H. Goldfine, AICHE J. **44**, 1923-1929 (1998).
[12] N. Lebleu, C. Roques, P. Aimar and C. Causserand, J. Membrane Sci. **326**, 178-185 (2009).

[13] M. Binz, A.P. Lee, C. Edwards and D.V. Nicolau, Microelectronic Engineering **87**, 810-813 (2010).
[14] R. Soto and R. Golestanian, Phys. Rev. E **89**, 012706 (2013).
[15] A. Costanzo, J. Elgeti, T. Auth, G. Gompper and M. Ripoll, Euro. Phys. Lett. **107**, 36003 (2014).
[16] A. Costanzo, R. Di Leonardo, G. Roucco, L. Angelani, J.Phys. Condens. Matter **24**, 065101 (2012).
[17] E.J. Harris, J. Appl. Prob. **2**, 323-338 (1965).
[18] P.S. Burada, P. Hanggi, F. Marchesoni, G. Schmid and P. Talkner, ChemPhysChem **10**, 45 (2009).
[19] Q.H. Wei, C. Bechinger and P. Leiderer, Science **287**, 625-627 (2000).
[20] M. Kollmann, Phys. Rev. Lett. **90**, 180602 (2003).
[21] Drescher K, Dunkel J. Cisneros L.H., Ganguly S. and Goldstein R.E., Proc. Nat. Acad. Sci. **108**, 10940-10945 (2011).
[22] A. Zöttl, H. Stark, Phys. Rev. Lett. **112**, 118101 (2014).
[23] B. ten Hagen, S. van Teeffelen and H. Lowen, J. Phys.: Condens. Matter **23**, 94119 (2011).
[24] H. Bruus, *Theoretical Microfluidics*, (Oxford University Press, 2008).
[25] J. Tailleur, M.E. Cates, Phys. Rev. Lett. **100**, 218103 (2008).
[26] M.E. Cates, Rep. Prog. Phys. **75**, 042601 (2012).
[27] L. Xie, T. Altindal, S. Chattopadhyay and X.L. Wu, Proc. Nat. Acad. Sci. **108**, 22462251 (2011).
[28] K.J. Duffy and R.M. Ford, J. Bacteriol. **179**, 14281430 (1997).
[29] J. Saragosti, P. Silberzan and A. Buguin, PLOSOne **7**, e35412 (2012).
[30] G. Rosser, A.G. Fletcher, D.A. Wilkinson, J.A. de Beyer, C.A. Yates, J.P. Armitage, P.K. Maini and R.U. Baker, PLOS Comp. Biol. **9**, e1003276 (2013).
[31] K. Drescher, K.C. Leptos and R.E. Goldstein, Rev. Sci. Instruments **80**, 014301 (2009).
[32] J.R. Howse, R.A.L. Jones, A.J. Ryan, T. Gough, R. Vafabakhsh and R. Golestanian, Phys. Rev. Lett. **99**, 048102 (2007).
[33] J.B. Delfau, C. Coste and M. Saint-Jean, Phys. Rev. E **84**, 011101 (2011).
[34] D.W. Jepsen, J. Math. Phys **6**, 405 (1965).
[35] C. Rodenbeck, J. Karger and K. Hahn, Phys. Rev. E **57**, 4382 (1998).
[36] G.S. Redner, M.F. Hagan and A. Baskaran, Phys. Rev. Lett. **110**, 055701 (2013).
[37] I. Theurkauff, C. Cottin-Bizonne, J. Palacci, C. Ybert and L. Bocquet, Phys. Rev. Lett. **108**, 268303 (2012).
[38] J. Palacci, S. Sacanna, A.P. Steinberg, D.J. Pine and P.M. Chaikin, Science **339**, 936-940 (2013).
[39] A.G. Thompson, J. Tailleur, M.E. Cates and R.A. Blythe, J. Stat. Mech.: Theory and Experiment P02029, (2011).
[40] B.M. Mognetti, A. Šarić, S. Angioletti-Uberti, A. Cacciuto, C. Valeriani and D. Frenkel, Phys. Rev. Lett. **111**, 245702 (2013).
[41] F. Peruani, A. Deutsch and M. Bär, Phys. Rev. E **74**, 030904 (2006).
[42] M.E. Cates and J. Tailleur *arxiv.org/pdf/1406.3533*, (2014).
[43] K. Wolff, A.M. Hahn, H. Stark, Euro. Phys. J. E **36**, 43 (2013).
[44] J. Tailleur and M.E. Cates, Euro. Phys. Lett. **86**, 60002 (2009).
[45] K. Grest and G.S. Kremer, Phys. Rev. A **33**, 3628 (1986).